Electrical transport properties of thin epitaxially grown iron films

Mark Rubinstein, F. J. Rachford, W. W. Fuller, and G. A. Prinz
Naval Research Laboratory, Washington, D.C. 20375-5000
(Received 26 August 1987)

We have determined the components of the magnetoresistance tensor through the fifth order in the magnetization direction cosines for four epitaxially grown iron films with thicknesses between 200 and 60 Å at 298, 77, and 4.2 K. We have also determined their magnetic anisotropy parameters, from ferromagnetic resonance, at room temperature. These phenomenological parameters provide an excellent description of the magnetic field dependence of the planar magnetoresistivity for electric current directed along the [100], [011], and [$\sqrt{2}$ 1 1] directions. The magnetization curves of iron films epitaxially grown on GaAs(110) show a first-order transition in the magnetization direction as a function of applied magnetic field. In addition to the single spin flops previously reported in such films, we have observed double spin flops in some of the films. The direction and magnitude of the applied field necessary to produce these consecutive magnetization reorientations have been calculated from the anisotropy parameters, and found to be in excellent agreement with experiment. We speculate that these transitions are caused by the formation and propagation of 90° domain walls. The low residual-resistivity ratios, the large spontaneous Hall coefficients, the likely appearance of conduction-electron localization, and the high resistivities of these iron films constitute evidence for the existence of a large defect density in Fe/GaAs(110).

I. INTRODUCTION

Since 1981 many papers have appeared which are concerned with the properties of thin iron films grown on GaAs substrates by molecular-beam epitaxy (MBE).[1] These papers reported on ferromagnetic resonance (FMR), magnetization, and electron-diffraction studies of single-crystal iron films. The studies were performed in order to determine the film quality and the magnetic properties of epitaxially grown thin iron films. These measurements revealed the existence of several unusual properties.

A first-order transition in the magnetization direction as a function of applied magnetic field was observed.[2] This transition was previously undetected in bulk iron samples, but it was readily observed in these films because the demagnetizing field constrained the magnetic moment to remain in the plane of the film.

The FMR measurements and superconducting quantum-interference device (SQUID) magnetometer measurements[3] revealed a dramatic and an as yet incompletely explained decrease in the magnetic moment per unit volume with decreasing film thickness from the bulk value $4\pi M = 21.5$ kOe.

In an attempt to investigate these epitaxially grown films further, we conducted electrical-transport measurements on a limited number of samples with iron-film thicknesses between 200 and 60 Å. The resistivity data of the present paper reveal that very thin films contain a high density of defects, while the Hall-effect data confirm their low magnetization. In addition, we have discovered two new effects: First, films with thicknesses less than approximately 100 Å show a resistivity minimum followed by a logarithmic increase of resistivity with temperature at low temperatures. This effect is tentatively interpreted as arising from localization and/or interaction effects. Second, we examined the field-induced "spin flops" in these thin iron films by monitoring the anisotropic magnetoresistivity caused by these abrupt changes in magnetization. In addition to the transition discovered by Prinz and Hathaway[2] in (110) plane of iron, a second spin-flop transition was observed as a function of increasing field when the magnetic field was applied in the plane of the film at angles between 90° and 120° from easy-magnetization [001] axis, in films whose thicknesses exceed 100 Å. A model which explains the existence of both sets of magnetic transitions is presented in this paper.

II. EXPERIMENT

Thin iron films were grown on GaAs substrates by MBE techniques. As in previously reported samples, the substrate orientation was chosen to be a (110) face. This face contains the magnetically easy [001], the hard [111], and the intermediate [110] directions of bulk iron, making it especially useful for magnetic studies. GaAs was chosen as the substrate because its nearest-neighbor distances are close (-1.4%) to that of bcc iron, and also because magnetic films deposited on semiconductors have application potential.

In order to make transport measurements on the iron films, it was necessary to use a highly insulating GaAs substrate. Most semi-insulating GaAs substrates are not electrically stable when heated in a high vacuum. Therefore, specially grown GaAs substrates were utilized. The substrates were cut from liquid-encapsulated Czochralski crystals that were doped with 6×10^{16} atoms cm^{-3} of chromium and 2×10^{16} atoms cm^{-3} of tin, which act as deep-level acceptor states. It was previously demonstrat-

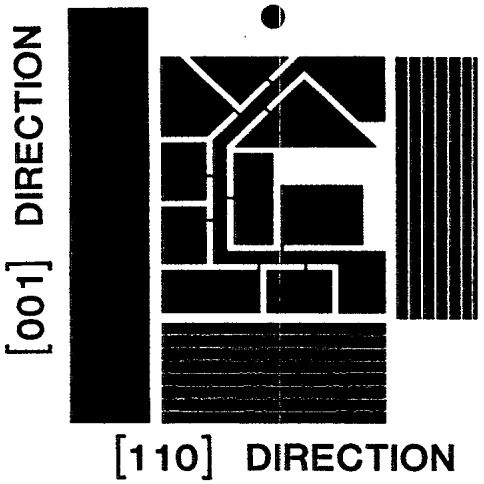

FIG. 1. Enlarged template used for photolithographic etching of the iron films. Conducting strips are along the [110], [001], and [$\sqrt{2}$11] axes. Copper leads are attached to pads by indium solder.

ed that these substrates are stable when heated to 740 °C for 90 min in flowing hydrogen.[4] These specially doped substrates did not convert, but remained highly insulating when heated at 625 °C in a vacuum for 30 min.

(110) substrates were prepared from this material using the conventional bromine method of polishing and etching procedures, followed by a 600-°C anneal in ultrahigh vacuum (UHV). The epitaxial growth of iron films on GaAs(110) has been described in previous publications.[5] Several samples were grown having iron thicknesses between 60 and 200 Å. These thicknesses were measured by x-ray fluorescence after the samples had been grown and removed from the vacuum chamber.

The samples were then photolithographically etched with a pattern of three conducting strips, one along the magnetically easy [001] axis, one along the [110] axis at a right angle to the [001] axis, and a third along an intermediate direction 45° from the [001] axis, as drawn in Fig. 1. Pads of Fe film connected to the conducting strips were left unetched, and copper wires were indium-soldered to these pads for electrical-transport measurements. The conducting strips were 3 mm long by 0.6 mm wide with a distance between the voltage leads of 2.1 mm. A fifth pad, in the center of the strip of iron film, was used as a contact for Hall-effect measurements. A strip of iron film was also left intact for subsequent analysis by FMR.

The samples were allowed to oxidize in air. It is believed that this produces a stable oxide surface of 30–35 Å, thus removing approximately 15 Å of metallic iron, and covering the remainder with a protective layer.[1]

III. SAMPLE CHARACTERIZATION

A. Ferromagnetic resonance (FMR)

Four samples of iron deposited on an insulating GaAs substrate were analyzed by FMR using the methods explained in previous publications.[1] The thicknesses of these samples were determined by x-ray fluorescence, and were measured to be 200, 160, 90, and 60 Å, respectively. The error in these values is estimated to be ±5 Å, but may be greater on account of the subsequent photolithography and etching. The 220- and 160-Å samples were found to have their easy direction of magnetization along the [001] axis, while the two thinner samples have their easy axis along the [110] direction. The thickness dependence of the anisotropy (presumably a competition between surface and bulk effects) has been observed in earlier work of this type. The samples are of single-domain type, and their magnetization lies in the plane of the film. In order to analyze the observed anisotropy of the FMR spectra, the following expression for the energy density was employed,

$$E=\mathbf{H}\cdot\mathbf{M}+K_1(\alpha_1^2\alpha_2^2+\alpha_2^2\alpha_3^2+\alpha_3^2\alpha_1^2)$$
$$+K_u\sin^2\theta+K_u'\sin^4\theta+2\pi M^2+K_\perp(M_\perp/M)\,, \qquad (1)$$

where θ is the angle between $\mathbf{M}$ and [001] in the (110) plane of the iron film, the α's are the direction cosines of $\mathbf{M}$ with respect to the cubic crystalline axes, and $M_\perp$ is the component of $\mathbf{M}$ normal to the surface and is used only when the field is applied normal to the film plane.

TABLE I. Phenomenological magnetic and electrical-transport parameters for several thin iron films used in this study. TA denotes tesla amperes.

Thickness (Å)	$4\pi M$[a] (kOe)	K_1/M[b] (kOe)	K_u/M[b] (kOe)	K_u'/M[b] (kOe)	R_o(300 K)[c] (V m/TA)	R_e(300 K)[c] (V m/TA)	ρ(300 K)[d] ($\mu\Omega$ cm)	RRR[e]
200	17.6	0.27	−0.22	+0.009	$+0.5\times10^{-10}$	$+23\times10^{-10}$	23.0	3.3
160	16.5	0.27	−0.05	+0.015			30.9	2.3
90	12.6	0.27	+0.35	−0.1			68.1	1.4
77							73.3	1.3
60	11.4	0.27	+0.63	−0.16	$+2.6\times10^{-10}$	880×10^{-10}	177.5	1.05
bulk	21	0.27	0	0	0.248×10^{-10}	6.33×10^{-10}	9.71	variable

[a]The value of $4\pi M$ is obtained from the extrapolation of the linear portions of Hall-voltage curves and is also in agreement with the ferromagnetic resonance data.
[b]K_1, K_u, and K_u' are obtained from fitting the angular dependence of the ferromagnetic resonance data.
[c]R_0 and R_e is the ordinary and extraordinary Hall coefficients obtained at room temperature (Rt).
[d]ρ(300 K) is the isotropic components of the resistivity tensor at 300 K.
[e]RRR is the residual-resistivity ratio (i.e., the ratio of the 300-K resistivity and the 4.2-K resistivity).

K_u and K_u' are the epitaxy-induced uniaxial in-plane anisotropy constants, and $K_\perp$ is the perpendicular anisotropy constant. Table I displays, among other values, the magnetic anisotropy and magnetization parameters deduced from FMR for these four films, and those for bulk iron at room temperature. Their dependence on film thickness is in agreement with previous studies. In particular, we note (1) the existence of a large uniaxial anisotropy attributed to the lattice mismatch between the GaAs and the Fe film, (2) the change in the easy direction of magnetization from [001] to [110] when the sample thickness is less than 100 Å, indicated by the change in sign of K_u, and (3) the low magnetization of the iron films compared to the magnetization of bulk iron at room temperature ($4\pi M \approx 21$ kOe). Further discussion of the FMR results is presented in a later section of this paper.

B. Resistivity

The resistivity of bulk iron at room temperature is 9.7 $\mu\Omega$ cm. The measured resistivity of the thin films discussed in this article greatly exceeds that of bulk iron. In Fig. 2 we have plotted the room-temperature resistivity of the iron films as a function of thickness (adjusted for a 15-Å-thick insulating oxide film) using the data tabulated in Table I. In Fig. 2 we have also plotted the thickness dependence of the resistivity predicted by the geometrical surface scatter theory of Fuchs-Sondheimer[6] assuming a mean free path at room temperature of 200 Å. It is clear that the measured resistivity departs markedly from the predictions of the Fuchs-Sondheimer theory, which postulates a bulk resistivity for the interior of the film and nonspecular surface scattering of electrons at the film's boundaries. This departure may be evidence that the enhanced resistivity is due to the presence of a large concentration of structural point or line defects in the film.[7] Prior to these measurements it was hoped that the epitaxially grown film would have a low resistivity due to their presumed crystalline perfection, although this reasoning has been questioned previously.[8] It now appears that the 1.4% lattice mismatch between bulk iron and bulk GaAs can produce a large number of defects which can propagate through a thin iron film. Diffusion of As atoms into the film near the GaAs/Fe interface is another mechanism which can increase the resistivity of ultrathin iron films. A very-fine-grained mosaic structure can cause similar effects.[8]

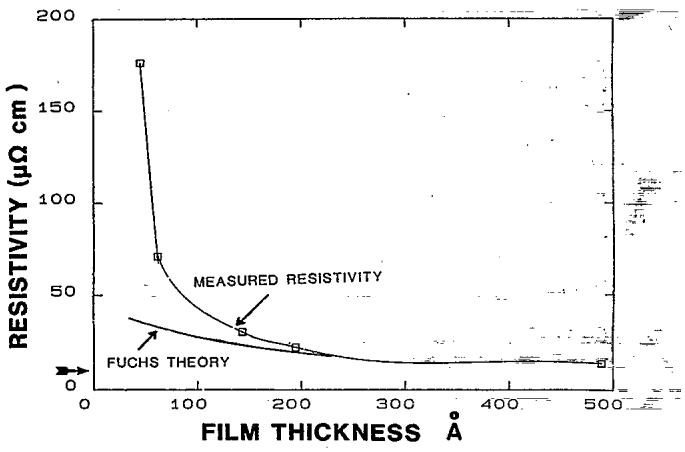

FIG. 2. Resistivity (in $\mu\Omega$ cm) at room temperature of iron films as a function of their thickness. The theoretical Fuchs-Sondheimer relationship, which postulates nonspecular scattering of electrons at film boundaries, is shown as a dotted line. The bulk iron value of room-temperature resistivity is indicated by an arrow.

C. Hall effect

The Hall resistivity of magnetic material, R_H, may be written as

$$R_H = R_o B + 4\pi R_e M_s \ , \tag{2}$$

where $B = H + 4\pi M$ and R_o and R_e are the ordinary and spontaneous Hall coefficients, respectively.[9] The values of R_o and R_e are shown in Table I for four thin iron films. The 60-Å-thick film has a much larger R_e than the 200-Å sample, indicative of its much higher resistivity.[9] For comparison, the values of R_o and R_e for bulk iron are also listed in Table I.

A plot of the Hall voltage as a function of the applied magnetic field for the 60-Å-thick film is shown in

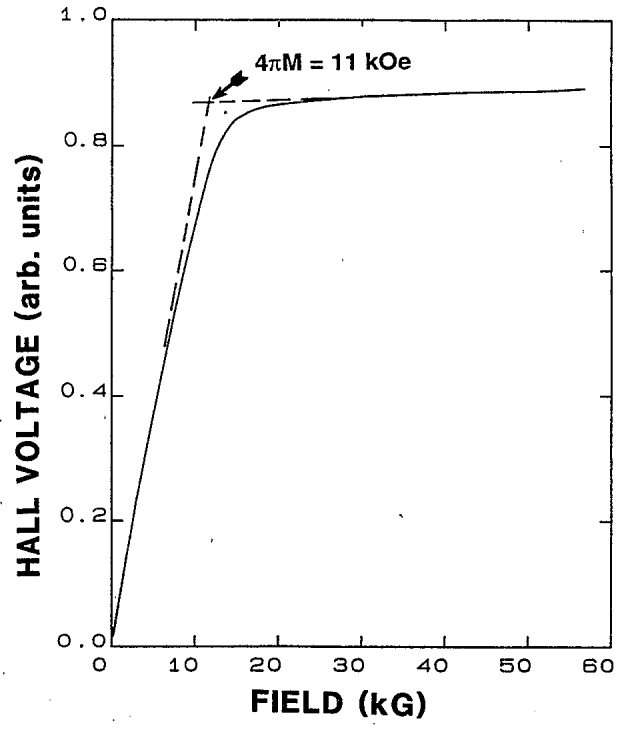

FIG. 3. Hall voltage in 60-Å-thick film as a function of applied magnetic field, at room temperature, with the magnetic field applied perpendicular to the plane of the film. The ordinary (terminal slope) and extraordinary (initial slope) Hall coefficients are given in Table I. The value of $4\pi M$ is obtained by determining the intersection of the linear regions of the ordinary and extraordinary Hall voltages. These values of magnetization agree with those derived from FMR, and are also given in Table I.

Fig. 3 with the construction used to obtain the apparent saturation moment $4\pi M$. From the extrapolation of the two linear portions of the Hall-voltage curves, we deduce $4\pi M = 11$ kOe for the 60-Å-thick film at 300 K, a value strongly reduced from the value for bulk iron (21 kOe), but in agreement with the FMR results for the same film. The deduced value of the saturation magnetization at room temperature may result, in part, from a reduction in the Curie point from the bulk value, a phenomenon often observed in thin magnetic films. However, even the value of the magnetization obtained at 4.2 K is greatly reduced in these films.[3] The value of $4\pi M$ deduced for the 200-Å-thick film from the Hall effect is much closer to the bulk iron value. The Hall-effect measurements substantiate the FMR and magnetization measurements, which display a large decrease in the magnetization per unit volume with decreasing film thickness. The apparent value of $4\pi M$ deduced by the Hall effect or by FMR is actually given by $4\pi M + 2K_\perp/M$, where $K_\perp$ is the perpendicular anisotropy constant. SQUID and vibrating-sample–magnetization measurements[1] reveal that the perpendicular anisotropy does not contribute to a significant reduction in the apparent value of $4\pi M$, and that the observed reduction in the magnetization of the thin film is a real phenomenon. It has been speculated that an Fe_2As compound is formed at the substrate interface,[1] with the As supplied by diffusion from the GaAs substrate.

D. Spin flops

Hathaway and Prinz[2] discovered the existence of a first-order magnetic phase transition in thin iron films with an [001] easy axis. Using a vibrating-sample magnetometer they observed that when a magnetic field is in the (110) plane of the iron film and aligned near the hard [110] axis, a sudden spin flop occurs with increasing field strength as the magnetization abruptly changes from being in alignment near the [001] axis to alignment near the [110] axis.

In our study we observed spin flops by monitoring the resistivity (or the planar Hall effect). The measurements were sensitive to such transitions due to the small but easily observed magnetoresistive anisotropy in the films. In addition to the single spin flops previously reported, we have observed double spin flops in some of the films. The double spin flops are closely related to the previously reported work, and can be calculated from a knowledge of the magnetocrystalline anisotropy parameters derived from our FMR experiments.

In Fig. 4(a) we have plotted the electrical resistance measured in the 160-Å-thick iron film as a function of ap-

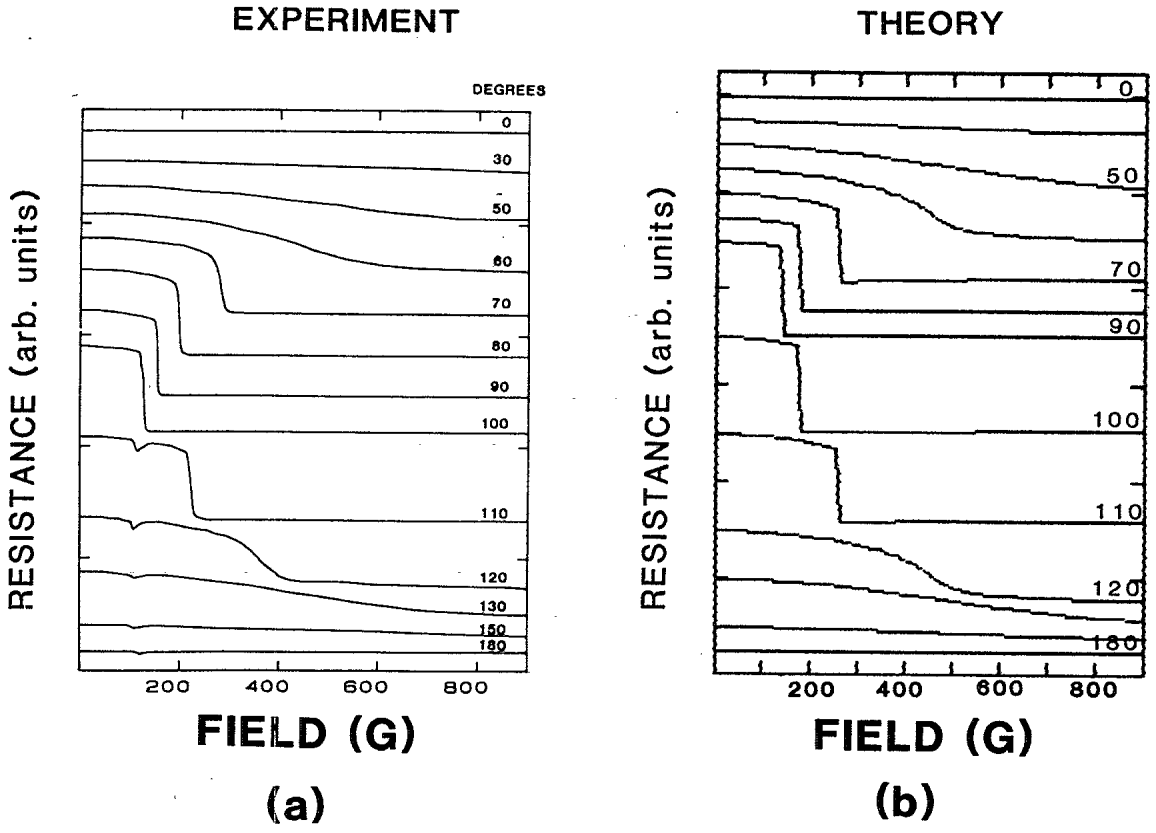

FIG. 4. (a) Experimentally determined resistivity vs applied magnetic field for various angles of the applied magnetic field in the 160-Å-thick film. The magnetic field is applied along the plane of the film with the current parallel to the [011] direction. The magnitude of the spin flops is predicted by the theory, and the small magnitude of some of them is due to the magnetization flopping by nearly 180°, where only small changes in the anisotropic resistivity result. (b) Theoretical family of magnetization curves as shown in (a).

plied magnetic field strength for a series of fixed angular orientations of the field with respect to the crystalline axis of the film. The direction of the current is along the [110] axis. The degrees displayed in Fig. 4(a) represent the angle in the (110) face between the easy [001] axis and the direction of the applied field. For example, the curve labeled "0°" is obtained while the field is aligned along the [001] axis, the curve labeled "90°" is obtained while the field is aligned along the [011] axis, and the curve labeled "180°" is obtained while the field is aligned along the $[00\bar{1}]$ axis. Initially, the film is poled with a strong magnetic field along the [001] axis, i.e., 0°.

For this film, abrupt changes in the resistivity as a function of applied field are observed whenever $\theta > 63°$. These changes are caused by spin-reorientation transitions which produce a sudden change in the electrical resistance because of a small (0.3%) anisotropic magnetoresistance in these iron films.

When $90° < \theta < 120°$ (for this one particular film) two magnetic-field-induced spin-reorientation transitions are seen, and when $\theta > 120°$ only a single transition is observed. The observations are valid only when the sample is initially magnetized along the easy axis, with the field initially oriented at 0°.

The behavior of the transition when $0° < \theta < 90°$ has already been discussed by Hathaway and Prinz[2] and by Krebs *et al.*[3] Neither of these papers investigated the behavior of single-crystal iron films when an external field is applied at angles greater than 90° from the easy axis. It is this region where double transitions are observed.

In Fig. 5 we plot the magnetic fields at which these single and double transitions occur versus field angle in the (110) plane for the 160-Å-thick iron film. The solid line is the theoretical prediction. The crosses are the experimentally observed values of the spin flop. The theory numerically calculates the magnetic energy [Eq. (1)] as a function of initial magnetization state, field amplitude, and orientation, and predicts the orientation of the magnetization. The region of double spin flops is indicated in Fig. 5.

To illustrate the origin of the spin flops and to relate the transition for $90° \leq \theta \leq 120°$ to the previously studied case where $63° \leq \theta \leq 90°$, we present a contour mapping of the energy surface for the magnetization as a function of magnetization angle in the (110) plane (relative to the [100] direction) and the applied field for the two symmetric cases where the external field is applied at 70°, Fig. 6(a), and at 120°, Fig. 6(b). At zero field, equal minima occur at the 0° and 180° positions corresponding to the equivalent cases where the magnetization is oriented along the [100] or $[00\bar{1}]$. The magnetization is assumed to be initially poled along the [001]. In Fig. 6(a), as the magnetic field is increased, the magnetization slowly rotates as the energy minimum shifts to a larger angle. At about 260 G the energy for an orientation at approximately 74° becomes less than the minimum near 24° and

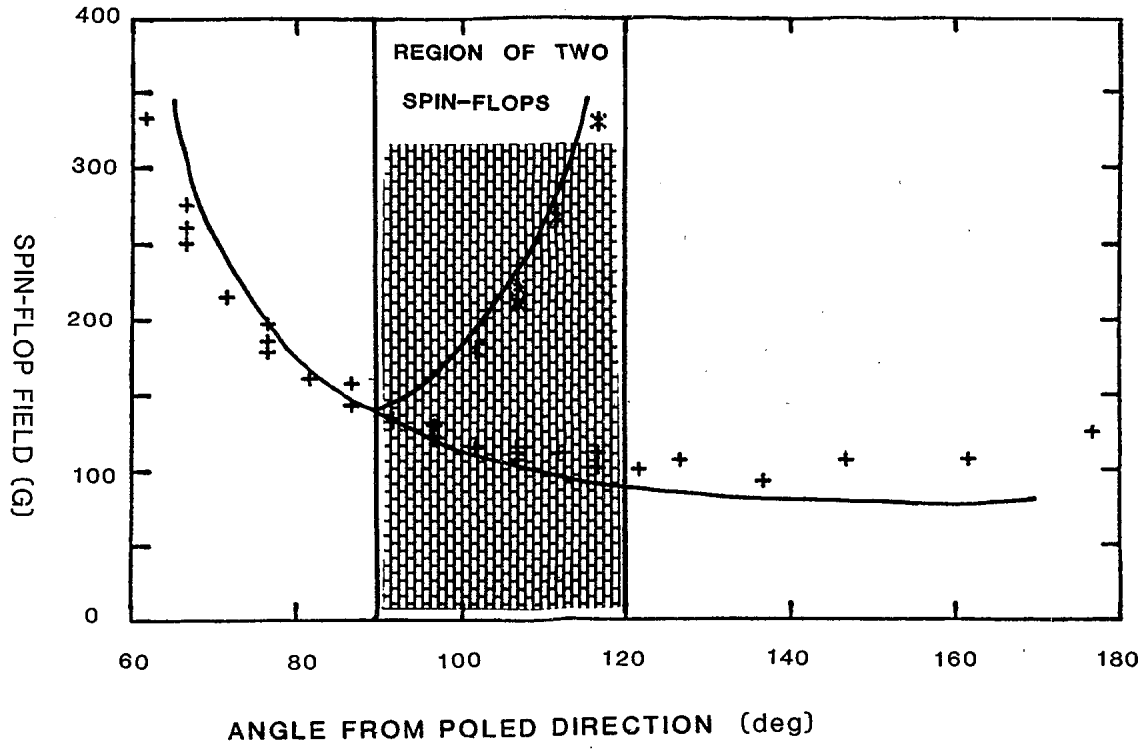

FIG. 5. Magnetic field amplitude, in Oe, at which spin flops are observed to occur for the 160-Å-thick iron film as a function of the angle of the field applied in the (011) plane, with the sample initially poled along the [011] axis. The solid lines are the theoretical values, while the pluses (+) and asterisks (*) represent the experimentally observed values. The regime of double spin flops, cross-hatched in the diagram, extends from 90° to 120° in this sample. Typical data are shown in Fig. 4.

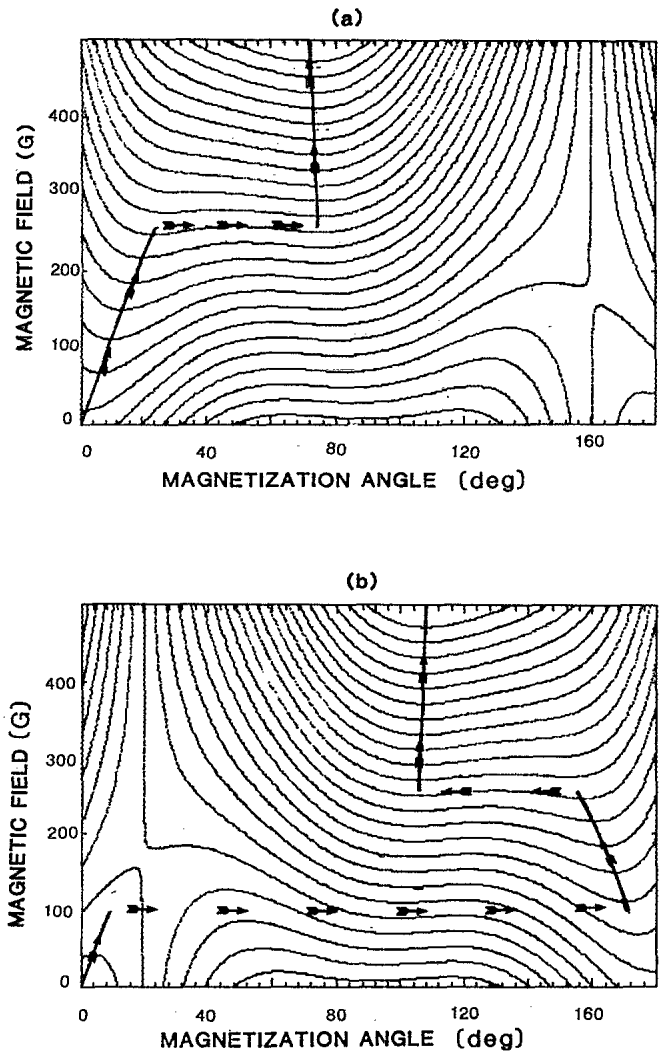

FIG. 6. The contours of energy vs magnetization angle and applied-field orientations in the (110) plane; (a) $\overline{H}$ applied at the 70° from the [100], and (b) H applied at 110° from the [100]. The trajectories of the magnetization orientation are indicated by the directed lines intersecting the energy contours. For case (a) only one magnetization reorientation occurs. For case (b) two reorientations occur.

the magnetization suddenly reorients. Here we neglect the domain-wall nucleation energy, and the magnetization-reorientation trajectory is theoretically reversible in applied fields, using this assumption. Experimentally, a small hysteresis is noted. This is an example of the previously studied magnetization reorientation transition.

In Fig. 6(b) we plot the case where the external field is applied at 110° to the [001]. The energy contours are mirror-reflected about 90° from those of the previous example. The magnetization is initially poled along the [001]. As soon as a magnetic field is applied, the global energy minimum is found near 180° [00$\bar{1}$]. We experimentally find that the magnetization does not immediately reorient to the global minimum, but remains in the local minimum near [001] until a transition to the energy minimum near the [110] becomes energetically favorable. At this point, we assume two ~90° walls are generated and sweep through the sample, reorienting the magnetization to the global minimum near the [110]. As the field increases further, the magnetization follows a trajectory which is the mirror image of the previous case [Fig. 6(a)]. The transition at ~100 G is not reversible and the magnetization rotates to the [001] as the field is subsequently reduced to zero.

Since reorientation is delayed until ~90 rotations are energetically favorable, we conclude that reorientations of greater than 90° occur by a two-step process, and large reorientations do not occur until "90°" walls can be generated. In this calculation we assume that the sample is of single-domain type, except during the magnetization reorientations when one or more 90° domain walls are generated and rapidly sweep through the sample.

Thus, using Eq. (1) and the parameters obtained from fitting the FMR data on each sample, we can numerically calculate the magnetic energy and generate an acceptable fit to the transition data. Due to the nature of the calculation, the calculated magnetization orientation is extremely sensitive to the values of the measured FMR parameters.

In order to reproduce the actual data traces we need to find the magnetoresistance tensor for the film. We do this by measuring the resistance in a large field as a function of angle in the plane assuming perfect alignment of **M** and **H** and negligible "forced" magnetoresistance. The high-field data are fitted to a fourth-order expansion of the magnetoresistance tensor in the direction cosines of the current direction and the direction cosines of the applied field (magnetization) with respect to the crystalline axis. With a knowledge of the magnetocrystalline anisotropy constants (obtained from FMR), we can reproduce the detailed shape of the resistance (and planar-Hall-effect) curves as a function of magnetic field. In Table II we list the magnetoresistivity tensor parameters deduced by measuring the sample resistivity at a saturating magnetic field, and then rotating the field for four iron films; no obvious trends are noticeable. Figure 4(b) shows the "theoretical" results for this sample [while the experimental results are shown in Fig. 4(a)].

The first spin flop is not apparent in Fig. 4(b), since the spin-flop transition involves a nearly 180° magnetization reversal which does not result in an appreciable change in the magnetoresistance. It is observable in Fig. 4(a) because of the finite speed with which the transition is transversed, and because of the simplification of the theory.

IV. PHENOMENOLOGY

In this section we describe in more detail how the parameters characterizing the magnetic and magnetorestrictive anisotropy are obtained, and how these parameters are utilized to predict the magnetization curves.

The magnetic anisotropy constants were obtained from FMR with the external magnetic field (H) applied in the

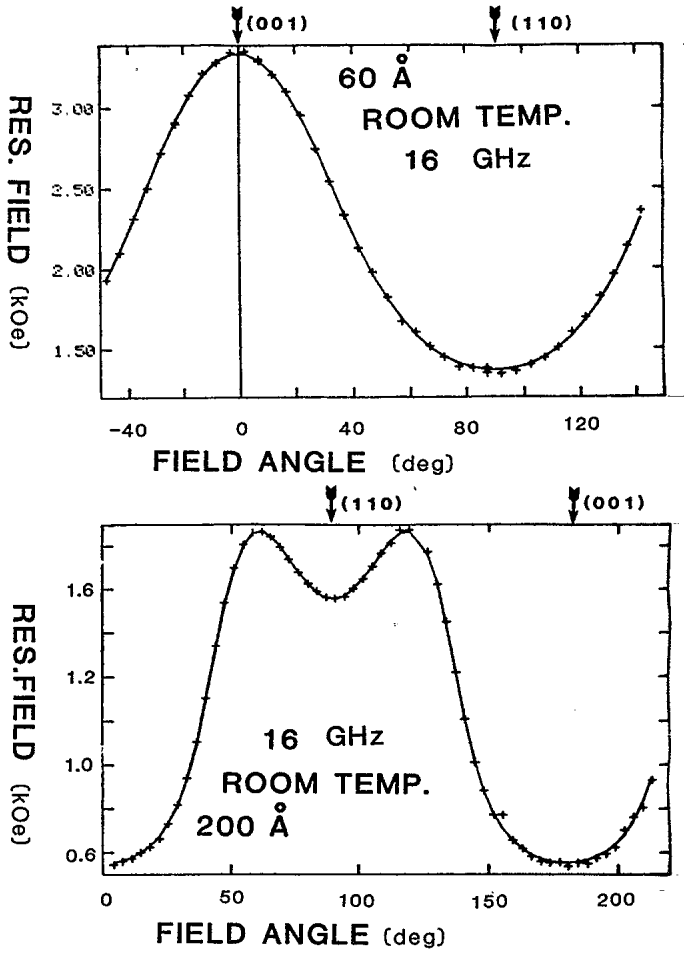

FIG. 7. Angular dependence of the external magnetic field necessary for ferromagnetic resonance in (a) an iron sample 60 Å thick and (b) an iron sample 200 Å thick.

plane of the film. The FMR lines, observed in a 16-GHz spectrometer at room temperature, are quite sharp, and the angular dependence of the resonance magnetic field can be graphed as a function of the angle (θ) between the [001] axis and the applied field. These plots are shown for two iron films 200 and 60 Å thick in Fig. 7.

The FMR data can be analyzed in terms of the energy density of a ferromagnetic film in a magnetic field given by Eq. (1). The resonance equations for the angular dependence of the uniform mode are obtained by using the equations of Suhl and Artman.[10] The magnetic anisotropy parameters are then found by a best-fit analysis to the angular dependence of the FMR field and are given in Table I. In Fig. 7 the experimental data are represented by pluses (+), while the solid lines represent the fit using the parameters in Table I. This method has been utilized previously in the study of similar iron films and in a recent article Krebs, Jonker, and Prinz[1] discuss the FMR analysis and cite many previous papers which used this technique.

In a magnetically saturated, single-crystal ferromagnet the magnetoresistance depends on the orientation of the internal magnetization. This is called the magnetoresistivity anisotropy effect, and has been described successfully by the use of phenomenological equations.[11] In such ferromagnets the resistivity $\overleftrightarrow{\rho}$ is a tensor

$$\mathbf{E}=\overleftrightarrow{\rho}\cdot\mathbf{J}\ , \tag{3}$$

where ρ reflects the magnetic symmetry of the crystal. For cubic iron, the cubic magnetoresistivity tensor[12] through fifth order in the magnetic direction cosines α is

TABLE II. Phenomenological magnetoresistance parameters at 300, 77, and 4.2 K for several thin iron films used in this study. Parameter of sample: all values are $\times 10^{-3}$, i.e., $-1.8=-1.8\times10^{-3}$.

Thickness (Å)	C_1	C_2	C_3	C_4	C_5	D_1	D_2
			Room Temperature				
200	+0.39	−1.53	−0.36	−4.98	−0.86	+1.27	−5.22
160	−1.80	−0.40	−1.06	+4.07	+0.78	−0.35	−1.94
93	+1.65	−0.19	+1.31	+3.28	−1.09	+1.96	+1.65
60	+1.90	+0.57	−0.46	−3.67	+1.97	+1.10	1.91
bulk[a]	+3.82	−1.76	+2.29	+5.93	+2.69	0	0
			77 K				
200	+3.38	−0.6	+7.1	+4.27	−2.6	+0.49	+2.07
160	−2.29	−0.9	+1.24	+2.14	+2.85	+1.26	−2.41
93	+1.87	−0.37	+1.66	+3.93	−1.58	+1.35	+1.26
60							
			4.2 K				
200							
160	−1.62	−2.56	+3.60	+0.35	+2.83	+3.16	−2.02
93	+1.09	−0.16	+0.67	+3.73	−0.72	+0.68	+1.05
60	+1.81	+0.74	−1.58	−5.17	+3.48	+0.04	+1.83

[a]Reference 13.

$$\rho^c=\begin{bmatrix} C_0+C_1\alpha_1^2+C_2\alpha_1^4+C_3\alpha_2^2\alpha_3^2 & C_4\alpha_1\alpha_2+C_5\alpha_1\alpha_2\alpha_3^2 & C_4\alpha_1\alpha_3\alpha_2^2+C_5\alpha_1\alpha_3\alpha_2^2 \\ C_4\alpha_1\alpha_2+C_5\alpha_1\alpha_2\alpha_3^2 & C_0+C_1\alpha_2^2+C_2\alpha_2^4+C_3\alpha_3^2\alpha_1^2 & C_4\alpha_2\alpha_3+C_5\alpha_2\alpha_3\alpha_1^2 \\ C_4\alpha_1\alpha_3+C_5\alpha_1\alpha_3\alpha_3^2 & C_4\alpha_2\alpha_3+C_5\alpha_2\alpha_3\alpha_1^2 & C_0+C_1\alpha_3^2+C_2\alpha_3^4+C_3\alpha_1^2\alpha_2^2 \end{bmatrix}. \quad (4)$$

In addition to the cubic tensor of Eq. (3), an orthorhombic perturbation ρ^o is necessary to describe the magnetoanisotropy of the iron films. This perturbation is created by the strained epitaxial bond of the film to the GaAs substrate, which creates an orthorhombic term in the resistivity tensor given by

$$\rho^o=\begin{bmatrix} D_1\alpha_1^2 & 0 & 0 \\ 0 & D_2\alpha_2^2 & 0 \\ 0 & 0 & 0 \end{bmatrix}. \quad (5)$$

The resistivity tensor is given by the sum of the cubic and orthorhombic matrices, $\rho=\rho^c+\rho^o$, and this tensor may be projected on the (110) plane for comparison with the experiment. In this plane $\alpha_1=\alpha_2=(1/\sqrt{2})\sin\theta$ and $\alpha_3=\cos\theta$. The cubic tensor is analogous to the cubic magnetic anisotropy term in Eq. (1), while the orthorhombic tensor is analogous to the uniaxial term. A more complete discussion of the magnetorestrictive origin of these noncubic terms is found in the paper by Krebs *et al.*[1] ρ^c and ρ^0 are given by Eqs. (4) and (5), and the parameters are given in Table II.

The components of the magnetorestrictive tensor were determined using the four-probe technique by measuring the resistance of three conducting iron strips photolithographically etched out of a thin MBE-grown iron film. The strips were directed along the [100], [011], and [$\sqrt{2}$ 1 1] directions. The angular dependence of the resistance along each of the three directions was measured with a field of 6 kOe directed along the film plane and rotated within this plane. The measurements were per-

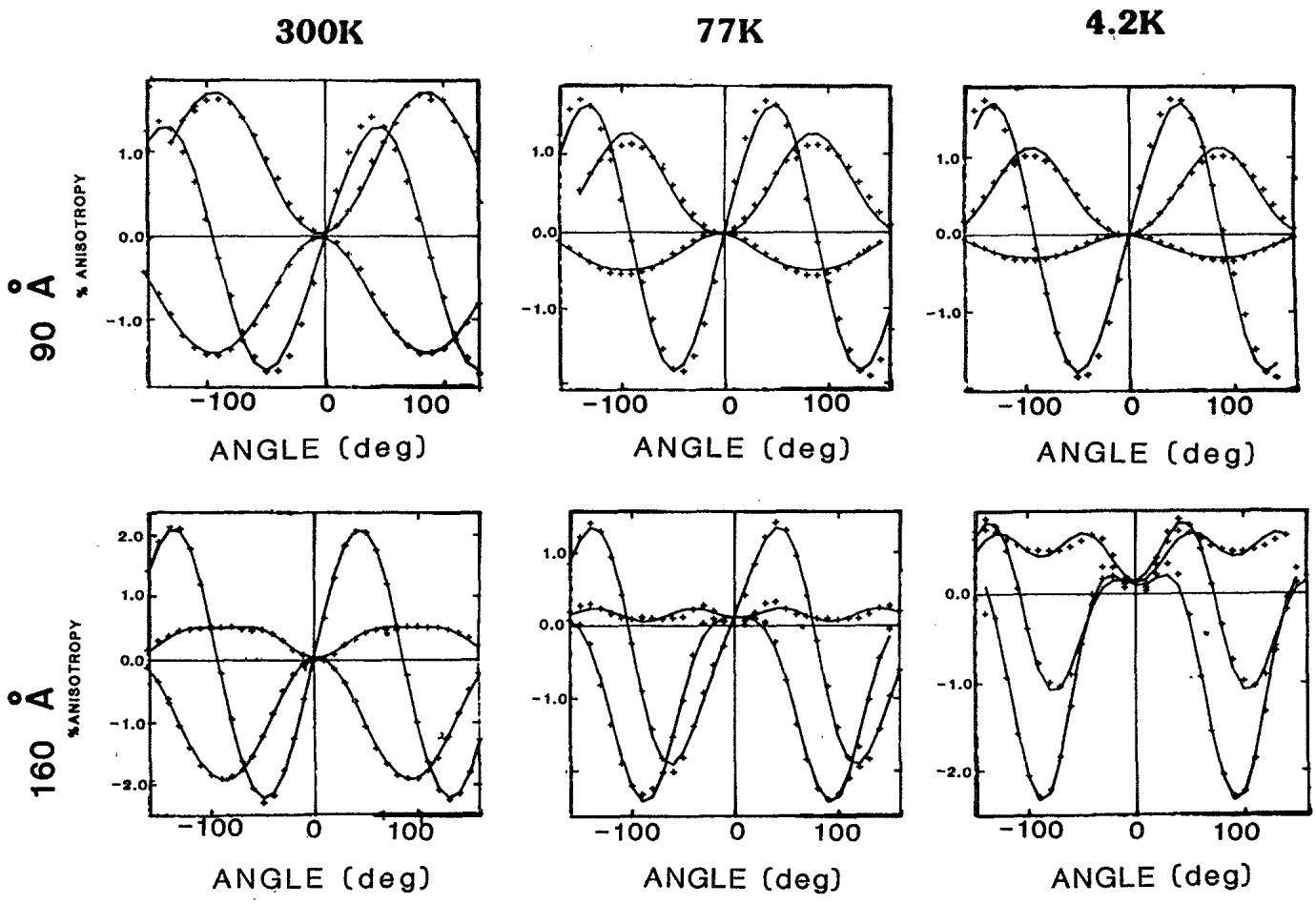

FIG. 8. Angular dependence of the planar magnetoresistivity for (a) a 60-Å-thick iron thin film and (b) a 160-Å-thick iron film. The data are shown for three temperatures: 300, 77, and 4.2 K. The three curves are those in which the current is along the [001], [110], and [$\sqrt{2}$11] directions, respectively. The applied magnetic field was set at 6000 Oe and rotated within the sample plane.

formed at room temperature, 77 K, and 4.2 K.

The angular dependence of the planar magnetoresistivity is shown in Fig. 8 for both a 160- and 90-Å-thick film. The calculated anisotropy coefficients based on the measured data in four iron films of varying thicknesses are shown in Table II. The bulk iron data of Hironi and Hori[13] are also given for comparison.

We have graphed the magnetization curves by measuring the resistivity of the strips as a function of angle between the magnetic field and the electrical current (with the magnetic field in the plane of the iron, as usual). The field is held at a constant direction and as the field is increased from zero, the magnetization rotates away from the easy axis and eventually aligns parallel to the applied field when this field exceeds the in-plane anisotropy field $2K_u/M$. The magnetization process is uncomplicated because the film is so thin that it is energetically favorable to eliminate the domain boundaries; the film is of single-domain type and the magnetization proceeds by single-domain rotation. For certain orientations of the applied field, spin flops occur, caused by the creation and motion of transient domain walls.

We obtain the experimental magnetization (or hysteresis) curves by initially poling the sample to saturation in the easy axis. The field is then reduced to zero and the magnet rotated so that its north-south axis forms an angle θ with the easy axis. The field is then gradually increased from zero, keeping the orientation constant,

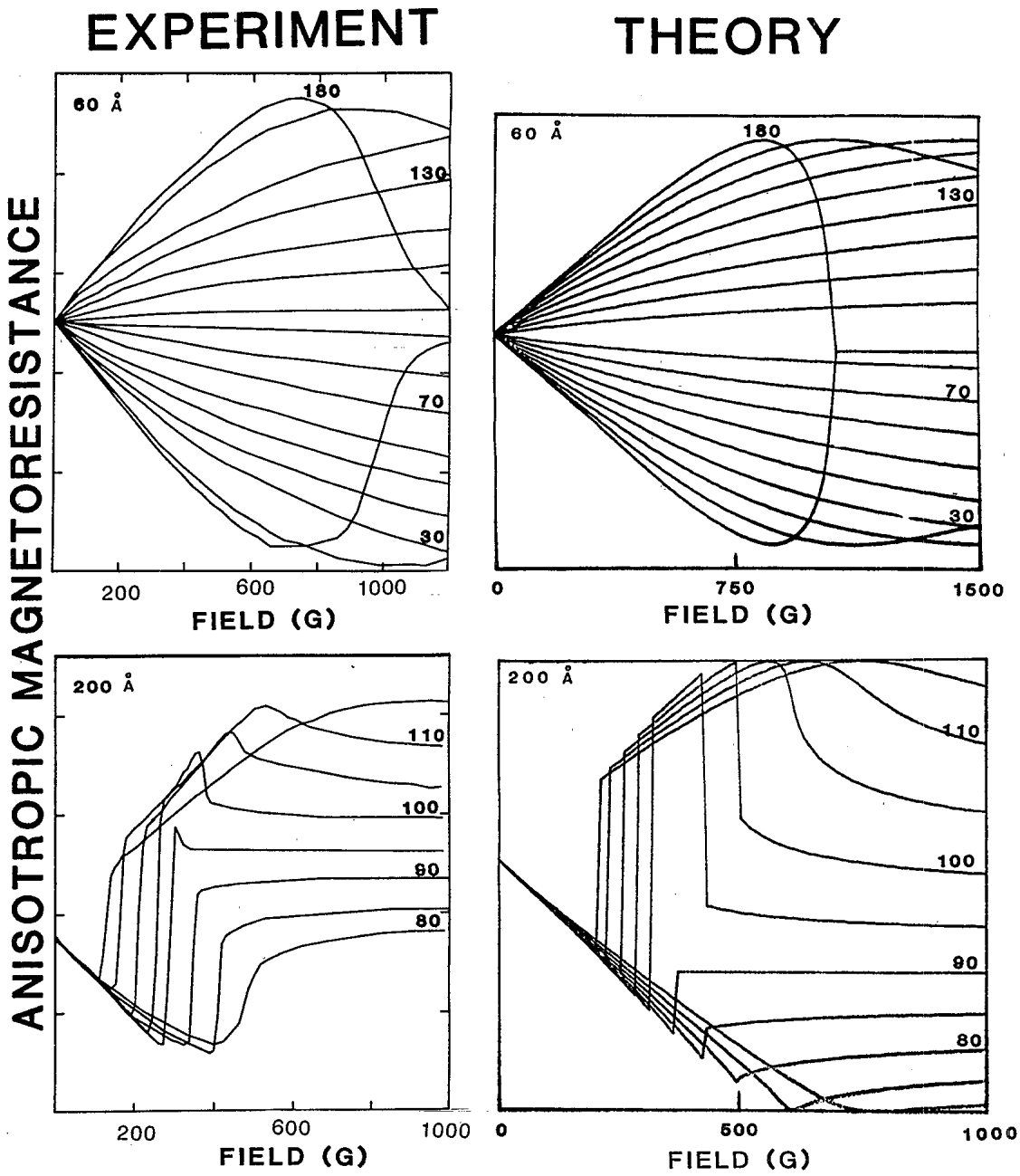

FIG. 9. The families of experimentally and theoretically determined magnetoresistance magnetization curves. Current is along the $[\sqrt{2}11]$ direction, while the field direction is given in degrees in the figures. Note the double spin flops in the 200-Å sample.

while the magnetoresistance of the iron strip is monitored. After the magnetization is clearly aligned along the field direction, the magnetic field is rotated back to the easy axis, and then reduced to zero. The field is then rotated to another θ, and the process is repeated. Two families of experimentally obtained magnetoresistance magnetization curves—the first for a 60-Å-thick film and the second for a 200-Å-thick film—are shown on the left-hand side of Fig. 9.

The angle θ is measured from the [001] axis, which is the magnetically easy axis for the 200-Å-thick sample, while the [110] is the easy axis for the 60-Å-thick film.[14] The current in both curves is along the $[\sqrt{2}11]$ axis, 45° from both the [100] and [011]. Similar curves have been obtained for the different current directions and film thicknesses. These curves reflect the rotation of the magnetization to alignment along the magnetic field, as monitored by the anisotropic resistivity as a function of increasing magnetic field. The near discontinuities in the data represent the spin flops discussed earlier.

It is possible to reconstruct the experimental curves of Fig. 9 by using the phenomenological magnetic anisotropy constants derived from FMR (Table I) and the phenomenological anisotropic magnetoresistive constants for each film (Table II) derived from the angular dependence of the magnetoresistance as shown in Fig. 8. We use the magnetic anisotropy constants K_1 and K_u to determine the angular orientation of the magnetization vector, and the magnetoresistive anisotropy constants (C_1, C_2, C_3, C_4, C_5, D_1, and D_2) to determine the corresponding resistivity change. The results of this procedure are shown along with the two experimental families of curves displayed in Fig. 9. The agreement between the phenomenological "theory" and the experiment is quite good. The discrepancy between the two can be attributed, in part, to the retention of the spontaneous magnetoresistance and the neglect of the forced (i.e., field-dependent) magnetoresistance.

V. LOCALIZATION AND INTERACTION EFFECTS

When the resistance of a 100-Å-thick iron film was measured as a function of temperature, a shallow minimum was found at approximately 15 K. This anomalous behavior stimulated a series of measurements on this and yet thinner samples. The resistance of the samples at low temperatures was measured using several methods: four-probe dc, low-frequency (33 Hz) ac, and an ac bridge. The typical measuring current was 1.0 μA. We found that over most of the temperature range (at least down to 0.7 K) the use of currents between 0.1 and 1.0 mA did not affect our results. A summary of our results is presented in Fig. 10, where resistivity as a function of temperature is plotted for two film thicknesses, 60 and 200 Å. As can be seen, the thicker sample does not show a resistive minimum. We also found that the temperature dependence did not depend on the orientation between the film's magnetization and the current. As the actual film thickness increases, the minimum appears to move to lower temperatures.

At 0.05 K a perpendicular magnetic field was applied

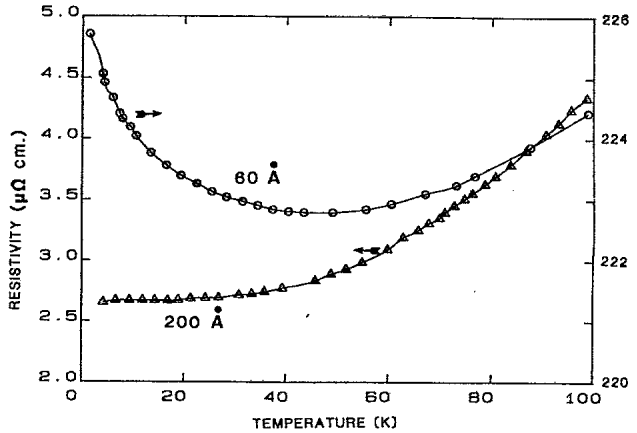

FIG. 10. Resistivity in $\mu\Omega$ cm as a function of temperature for the 60- and 200-Å-thick samples. The 60-Å-thick film has resistivity minimum of 45 K, while the 200-Å-thick film does not have a resistivity minimum. Intermediate thicknesses show minima at lower temperatures.

to the 75-Å-thick film. With the current in either the [110] or [001] direction, no magnetoresistance (to 0.05%) was seen for applied fields up to 600 G; thus the temperature dependence of the resistance is not affected by low magnetic fields.

In recent years many nonmagnetic thin films which have resistive minima have been studied in terms of electron-localization and/or electron-interaction effects.[15] One might not expect an Fe film to exhibit localization, since the conduction electrons experience such a large internal magnetic field, $4\pi M = 21$ kG, as determined from de Haas–van Alphen experiments. Magnetic fields of this magnitude delocalize the electrons through the formation of cyclotron orbits. However, in this case the internal field and the sample magnetization are in the plane of the films and, thus, due to the thinness of the films, the delocalizing orbits cannot exist. A recent paper on localization effects in itinerant ferromagnets show that the localization correction for the dc conductivity is unaffected by the magnetization.[16]

In Fig. 11 we have plotted $\sigma(T)-\sigma(T_0)$ versus $\ln T$, where σ is the conductance per square and T_0 is the temperature at the resistance minimum. As can be seen, the result is linear over several decades of temperature for the films showing a resistivity minimum, and the $\Delta\sigma$'s per decade of temperature are all close to 2.9×10^{-5}. The theoretical expression for the conductivity in a two-dimensional localized film is $\Delta\sigma = \xi\alpha \ln(T/T_0)$ $= 2.3\xi\alpha \log_{10}(T/T_0)$, where $\Delta\sigma = \sigma(T)-\sigma(T_0)$, $\xi = e^2/2\pi^2 = 1.23\times10^{-5}\ \Omega^{-1}$, and α is a number of order unity.[10] When $\alpha = 1$ the theoretical prediction for $\Delta\sigma$ per decade of temperature is 2.8×10^{-5}. If it is permissible to apply this theory to ferromagnetic iron, our data yield an α very close to 1.0. This expression arises from both the electron-localization and electron-electron–interaction picture. To distinguish between the two effects, the magnetoresistance and the Hall effect must be measured; at least this is so in nonmagnetic films. To use the magnetoresistance to distinguish between the two effects, one must be able to separate the magne-

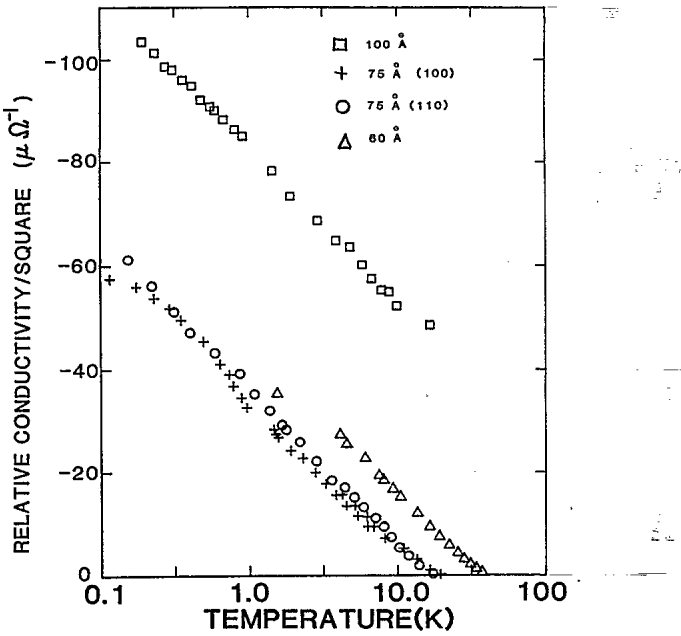

FIG. 11. Conductivity vs $\log_{10}(T)$ for several film thicknesses less than 100 Å. Measurements were made in a dilution refrigerator. The conductivity varies logarithmically with temperature over several decades of temperature, and the changes in conductivity per decade of temperature are all very close to 2.9×10^{-5} Ω^{-1}, the values predicted by either the two-dimensional localization theory or the two-dimensional interaction theory.

toresistance due to the magnetic material from that due to localization or interaction effects. In the high-field limit, which is where it is easiest to distinguish between the interaction and localization pictures, we observed a negative magnetoresistance at 4.2 K. Between 30 and 130 kG it appears to be linear with field. (Bulk iron exhibits a positive magnetoresistance at this temperature.) The localization (interaction) picture predicts a $-\ln H$ ($+\ln H$) dependence at high fields;[10] thus, there is some other effect that is dominating the magnetoresistance in these iron films. Thus far, most theories have not considered magnetic thin films where exchange interactions dominate; one paper[16] discusses localization in magnetic films but does not consider the Hall effect, magnetoresistance, or the effects of the simultaneous existence of *s* and *d* bands. Previously, magnetic Ni films have been reported by other authors to exhibit an $\ln T$ conductivity and weak, negative magnetoresistance.[17]

The temperature dependence of the Hall resistance is another way to distinguish between the effects of localization and electron-electron interaction. For localization in nonmagnetic metals there should be no temperature dependence, while in the electron-electron–interaction picture the change in the Hall resistance between two temperatures should be twice the change in the normal zero-field resistance between the same temperatures.[15] To measure the ordinary Hall resistance in iron, one must utilize high fields (>30 kG) since iron shows an anomalous Hall effect at lower fields. We found that for the 60-Å-thick film the zero-field resistance increased by $\approx0.3\%$ between 4.2 and 15 K. The Hall resistance also appears to have changed slightly, but not definitively [$(1.0\pm1.0)\%$]. Thus, from the Hall measurements one cannot distinguish between the localization and electron-interaction theories for our samples. We can say that the Hall-resistance results are not inconsistent with either theory.

A resistive minimum and the subsequent logarithmic increase may be explained either by the localization and/or interaction theories discussed above or by the Kondo effect. The Kondo effect involves a spin-flip scattering of electrons by magnetic impurities; thus a Kondo effect would not be expected in a magnetic material (but can exist in amorphous or highly inhomogeneous magnets).[18] Also, the Kondo effect is a bulk effect and thus should be less important as the film becomes thinner and surface scattering increases. Our films show that the temperature of the resistivity minimum increases as the film thickness decreases and, therefore, a magnetic Kondo effect is unlikely to explain observed behavior.

VI. CONCLUSION

The low residual-resistivity ratios, the large spontaneous Hall coefficients, the (presumed) appearance of conduction-electron localization, and the high room-temperature resistivities of these thin iron films constitute evidence for the existence of a large defect density in Fe/GaAs(110). This is a plausible conclusion in light of the photoemission studies on Fe/GaAs(110) by Ruckman, Joyce, and Weaver,[19] which indicate that extended interdiffusion and chemical reaction between Fe, Ga, and As occur, and the x-ray studies of Qadri *et al.*,[8] which reveal the existence of a very-fine-grained mosaic structure.

The dramatic decrease in the magnetic moment per unit volume with decreasing film thickness appears to have a rather mundane explanation. Chemical reactions at the interface and diffusion of As into the Fe film may produce antiferromagnetic Fe-As compounds, and also dilute the Fe concentration near the interface, while maintaining the epitaxy. Thus, the thinner samples possess a lower average magnetic moment, since proportionately more sample is near the GaAs/Fe interface.

Resistivity measurements (or possible Hall-effect or magnetization measurements) offer the feasibility of a determination of the defect density for manufacturing quality control.

The magnetic anisotropy, and the components of the magnetoresistance tensor, have been determined as functions of temperature and film thickness. The parameters provide a very good description of the magnetoresistance magnetization curves.

In addition to the single spin flops previously reported in Fe/GaAs films, we have observed double spin flops in

some of the films. The direction and magnitude of the applied field necessary to produce these spin flops have been calculated from the magnetic anisotropy parameters obtained by FMR, using a specific assumption concerning the conditions whereby a domain wall will sweep through the sample, and were found to be in agreement with experiment.

ACKNOWLEDGMENTS

We wish to thank Dr. J. Stannard for patterning the iron films, Mr. E. Swiggard for providing the doped GaAs insulating substrates, and Dr. G. H. Stauss for assisting in the theoretical interpretation.

[1]J. J. Krebs, F. J. Rachford, P. Lubitz, and G. A. Prinz, J. Appl. Phys. **53**, 8058 (1982), and references therein; J. J. Krebs, B. T. Jonker, and G. A. Prinz, *ibid.* **6**, 2596 (1987), and references therein.

[2]K. B. Hathaway and G. A. Prinz, Phys. Rev. Lett. **47**, 1761 (1981); F. J. Rachford, G. A. Prinz, J. J. Krebs, and K. B. Hathaway, J. Appl. Phys. **53**, 7966 (1982).

[3]J. J. Krebs, F. J. Rachford, P. Lubitz, and G. A. Prinz, J. Appl. Phys. **53**, 8058 (1982).

[4]E. M. Swiggard, S. H. Lee, and F. W. VonBatchelder, in *Gallium Arsenide and Related Compounds—1978,* Inst. Phys. Conf. Ser. No. 45 (IOP, Bristol, 1979), p. 125.

[5]G. A. Prinz, J. M. Ferrari, and M. Goldenberg, Appl. Phys. Lett. **40**, 1551 (1982); G. A. Prinz and J. J. Krebs, *ibid.* **39**, 397 (1981).

[6]E. H. Fuchs-Sondheimer, Adv. Phys. **1**, 1 (1952).

[7]R. Suri, A. P. Thakoor, and K. L. Chopra, J. Appl. Phys. **46**, 2574 (1975).

[8]S. B. Qadri, G. A. Prinz, J. M. Ferrari, and M. Goldenberg, J. Vac. Sci. Technol. B **3**, 718 (1985); S. A. Chambers, F. Xu, H. W. Chen, I. M. Vitomirov, S. B. Anderson, and J. H. Weaver, Phys. Rev. B **15**, 6605 (1986).

[9]S. M. Hurd, *The Hall Effect in Metals and Alloys* (Plenum, New York, 1972), p. 153.

[10]H. Suhl, Phys. Rev. **97**, 544 (1954); J. O. Artman, *ibid.* **105**, 74 (1957).

[11]W. Doring, Am. J. Phys. **33**, 259 (1938).

[12]R. S. Birss, *Symmetry and Magnetism* (North-Holland, Amsterdam, 1964).

[13]T. Hironi and N. Hori, Sci. Rep. Takahu Imp. Univ. **30**, 125 (1945), quoted by R. M. Bozorth, *Ferromagnetism* (Van Nostrand, New York, 1951), p. 767.

[14]G. A. Prinz, G. T. Rado, and J. J. Krebs, J. Appl. Phys. **53**, 2089 (1982).

[15]P. A. Lee and T. V. Ramarkishnan, Rev. Mod. Phys. **57**, 287 (1985); G. Bergman, Phys. Rep. **107**, 1 (1984).

[16]A. Singh and E. Fradkin, Phys. Rev. B **35**, 6894 (1987).

[17]S. Kobayashi, Y. Ootuka, F. Komori, and W. Sasaki, J. Phys. Soc. Jpn. **51**, 689 (1982).

[18]G. S. Grest and S. R. Nagel, Phys. Rev. B **19**, 357 (1979).

[19]M. W. Ruckman, J. J. Joyce, and J. H. Weaver, Phys. Rev. B **33**, 7029 (1987).